

The high Cu concentration zones are distributed from the central part of The Old Alaska mine to the northern part of the Greenshields farm and the eastern part of the Alaska farm. These high Cu concentration zones correspond to the basic dyke in the southern part of the mine, and the dolomite of Lomagundi Group in the western part of the mine. In addition to these characteristics, waste dumps are scattered around the mine and waste ores also are spottedly left in the farms.

2) The successive high Cu concentration zones from Greenshields farm, The Goldenvale farm, the Belltrees farm and the Freda farm

These narrow continuous high Cu concentration zones correspond to the basic dykes in the northern part of the site. There is no corresponding basic dykes exposure in the southern part, however, there could be extensions of the dykes.

3) The high Cu concentration zone from the Alaska smelter to the Sinoia Drift Estates farm

The high Cu concentration zone is widely distributed from the Alaska smelter to the Sinoia Drift Estate. This high Cu concentration zone neither shows any geological trend nor geological structure. Waste ore was left in the southern part of the smelter, and there is no facilities for flue gas treatment.

4) The high Cu concentration zone from Angwa Mine to the Hans Mine

The medium to small scale high Cu concentration zones successively continue from the Angwa mine to the Hans mine. Both the mines are included in the high Cu concentration zone. These high Cu concentration zones have two trends (NE-SW and NNW-SSE). These two directions correspond to the direction of the strike, fold axis and fault zone of this site.

1-3. Consideration

1-3-1. Comparison of the results of geochemical survey of Phase I and the analyses of previous geochemical data of 1993

The analyses of previous geochemical data are summarised in Fig.II-1-4.

The anomalous zones due to the Cu-Ag-Au mineralisation of this area are considered to be the following three places by 1992's geochemical survey:

- 1) The distribution area of arkose of the Deweras group**
- 2) The high Cu concentration zone of single component of Cu**
- 3) The high scoring places of the 4th component by principal component analysis used the six components of Cu, Pb, Zn, Fe, Co, Ni**

The anomalous zones selected by the above conditions were compared to and supplemented to compare to the existing data analyses of this year.

1. The Greenfields area

The high Cu concentration zone of this area corresponds well to the 1992's study results.

1) The central to southern part of the Wolwehoek farm

This site was not decided to be a mineralised anomaly, as a result of the low scoring of the principal component analysis of 1992's study. It was known that the distribution area of the Lomagundi group and the basic intrusives show high Cu concentration anomaly without mineralisation. This high Cu concentration zone is not due to mineralisation but is a reflection of geological conditions.

2) The central to northern part of the Chimusenga farm

This site slightly satisfied the above three conditions, and was considered to be a mineralisation anomaly by 1992's study. On the other hand, it corresponds to the small scale basic intrusives. Almost the same high Cu concentration zone was detected by 1993's survey. This high Cu concentration zone is considered to be formed by both the mineralisation and basic intrusives.

3) The western part of the Greenfields farm

The high Cu concentration zone shows rather wide distribution by 1992's study. It was considered to be a mineralisation anomaly because of the satisfaction of the three conditions. Small scale high Cu concentration zones which correspond to the anomalous zone were detected by 1993's survey. These high Cu concentration zones correspond to the mineralisation layer of the Mhangura mine which is considered to be formed by the mineralisation.

4) The Geduld farm

This site shows low scoring of the principal component analysis, and was not considered to be a mineralisation anomaly. The wider high Cu concentration zone was detected by 1993's survey. This zone is considered to be due to by basic intrusives.

5) The Chirombozi farm

The anomalous zones located in the western side of the main road are rather wide, and the small scale anomalous zones are located in the eastern side of the main road. The high Cu concentration detected by 1993's survey is considered to be due to the mineralisation and basic intrusives. The high Cu concentration zone of the eastern side which is located in the boundary

area of the arkose and the granites is also due to mineralisation and has a probability of being on an ore-deposit.

2. The Piringani area

The existence of two high Cu concentrations were considered by the results of last year's study. The high Cu concentration zone is located in the southern part of the Norah mine. It is considered to be due to mineralisation.

3. The Inyati area

Comparatively wide high anomalous zones were detected by 1992's study. The anomalous mineralisation zone is located in the northern part of the mine and was detected by the results of principal component analyses. The high Cu concentration zone can be divided into two parts according to 1993's study. One corresponds to dolomite of the Lomagundi group which shows high Cu concentration. The other, whose scale is small, corresponds to the distribution of basic dykes and quartz vein of the central area. The high Cu concentration zone of the central part is considered to be due to the basic intrusives and mineralisation, however, the scale is very small.

4. The Lions Den area

Only one anomaly was detected by the year's study. The feature of the high Cu concentration zone is clarified by 1993's survey. This high Cu concentration zone which is narrowly elongated shows characteristic distribution due to the basic dykes of this area.

5. The Angwa area

1) The wide high Cu concentration zone around the Old Alaska mine

The distribution of the high Cu concentration by 1992's study shows the same distribution by this year's survey. The mineralisation anomaly is limited around the mine. The high Cu concentration zone of Cu which was detected by 1993's survey is considered to be due to by the complicated activities of dolomite of the Lomagundi group, basic intrusives, waste ores and mineralisation.

2) The successive high Cu concentration zone in the Greenshields farm, the western part of the Goldenvale farm, the Belltrees farm and the Freda farm, and the high Cu concentration zone in the western part of Freda farm

This zone was not considered to be a mineralisation zone because of the low scoring of the principal component analysis. This narrow and successive zone shows the characteristic distribution by the mafic dyke. It cannot be considered to be a high Cu concentration zone due to mineralisation.

3) The high Cu concentration zone from the Alaska smelter to the Sinoia Drift Estate

Two anomalies were detected by 1992's study. The high Cu concentration zone of Cu distributes approximately from east to west in broad width. It can be considered to be due to littering during ore-dressing, and difficult to be due to mineralisation.

4) The high Cu concentration zone from the Angwa to the Hans Mine

The high Cu concentration zones were detected in the southern part of Angwa mine and the northern part of Hans mine by 1992's study. Surrounding these zones, the high Cu concentration zone is widely distributed. A clear trend was detected in the direction of the strike, fold axis, fault zone and the successive direction of the ore deposits of this site by 1993's survey. This high Cu concentration zone is considered to be possibly due to mineralisation.

1-3-1. The other geochemical anomalies

The other geochemical anomalies were detected in the northern part of the Greenfields site(the Wilden farm) and Binge site(the Chipiri farm, the Tchetchenini farm, the Binge farm and the Redwing farm) by 1992's study. No geochemical survey has been carried out in this site, all these detections are completely new facts.

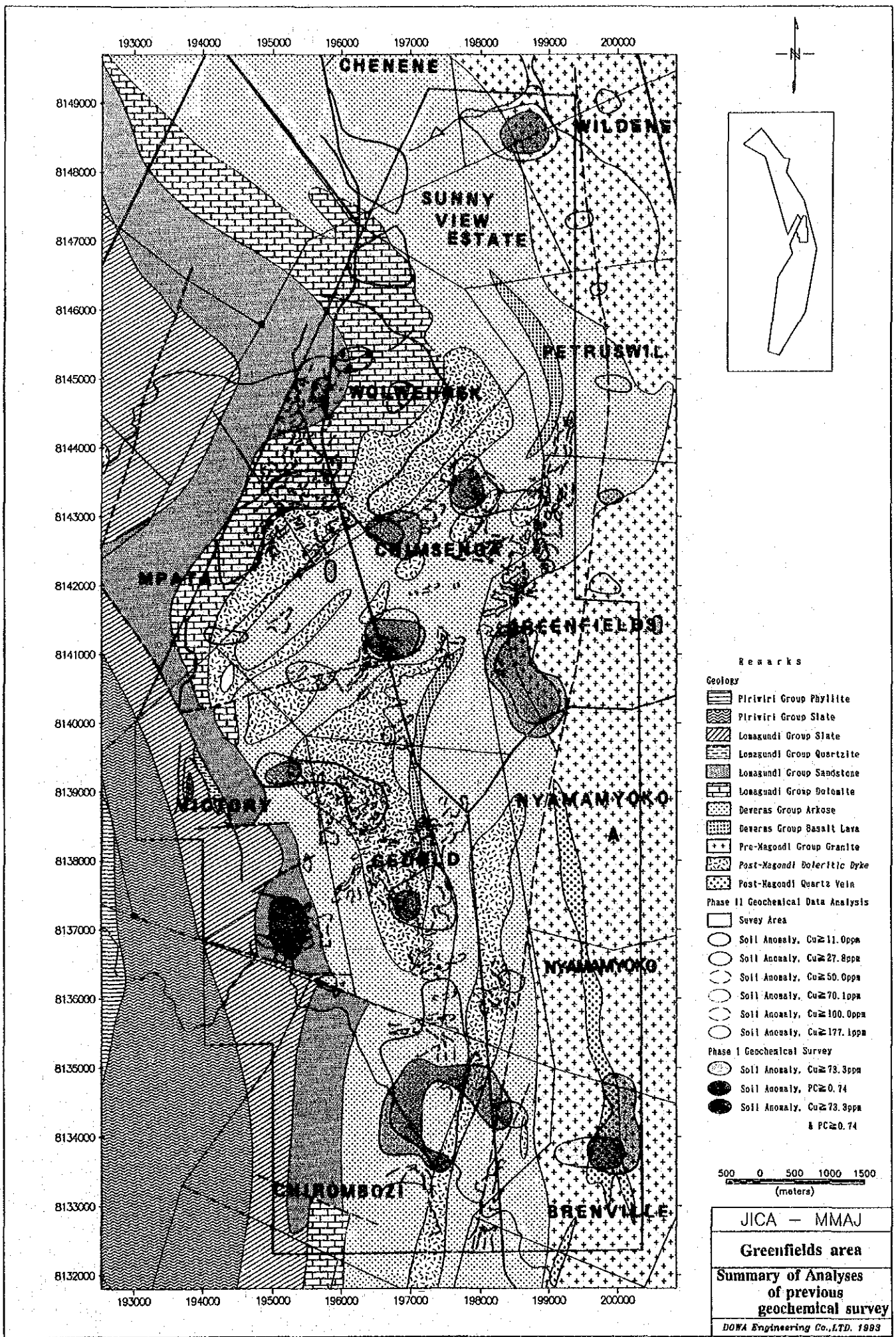


Fig.II-1-4 Summary of the analyses of previous geochemical survey (Greenfields area)

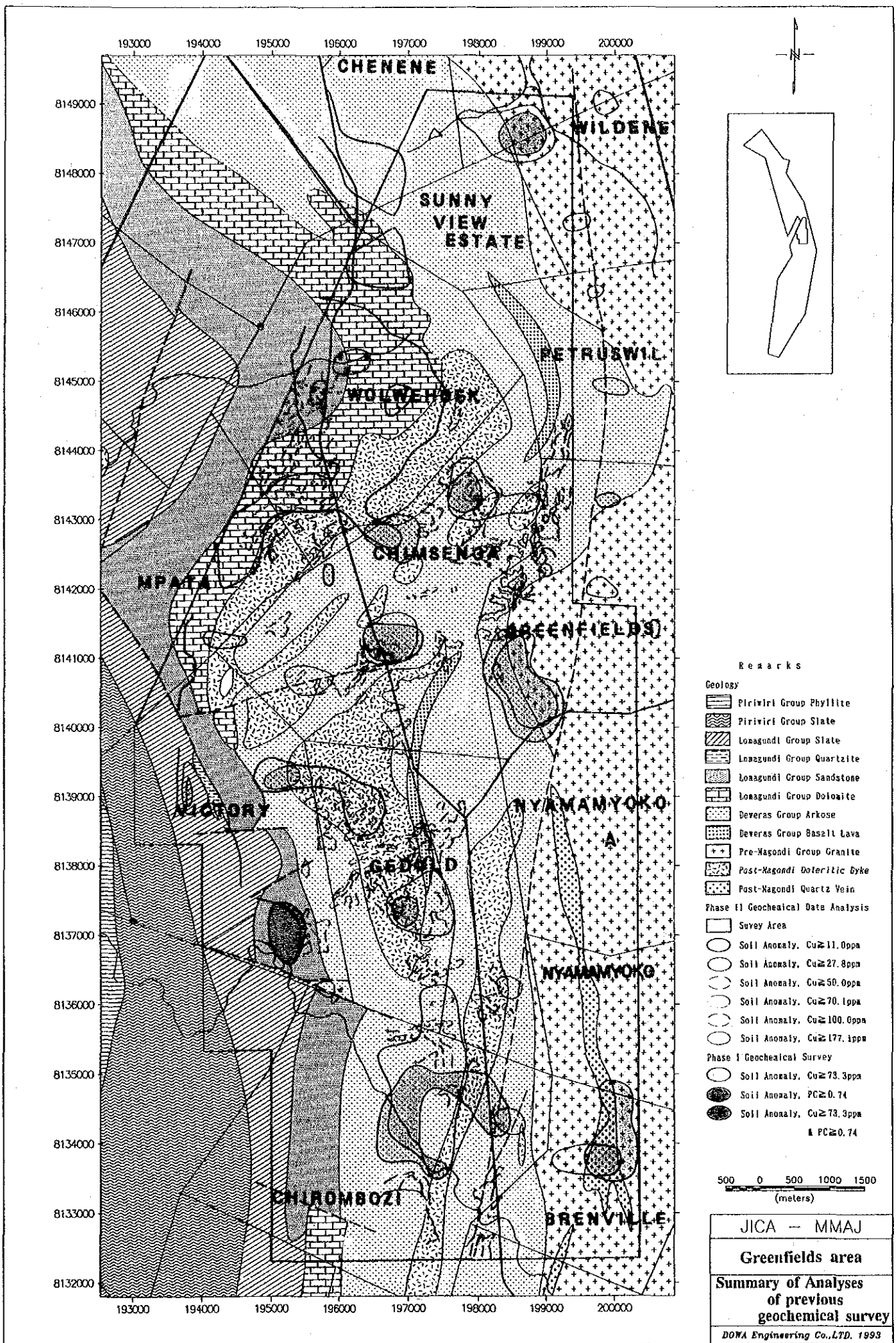
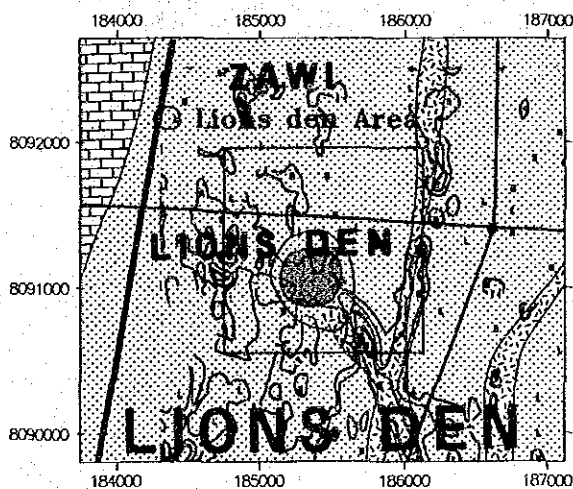
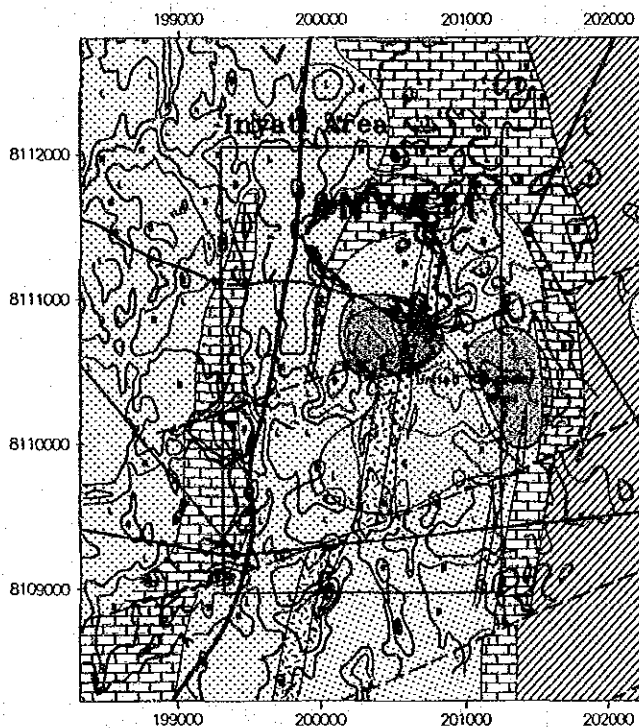
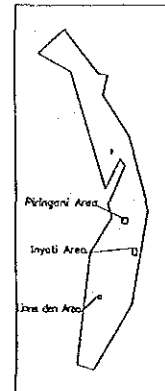
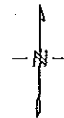
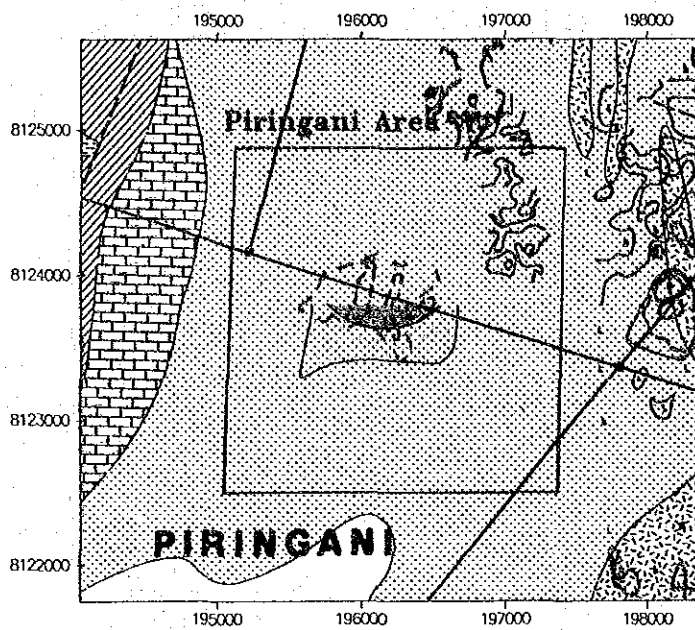


Fig.II-1-4 Summary of the analyses of previous geochemical survey (Greenfields area)



- Remarks
- Geology
- Lowagundi Group Slate
 - Lowagundi Group Sandstone
 - Lowagundi Group Dolomite
 - Deveras Group Arkose
 - Post-Magondi Doleritic Dyke
 - Post-Magondi Quartz Vein
- Phase II Geochemical Data Analysis
- Survey Area
 - Soil Anomaly, Cu \geq 11.0ppm
 - Soil Anomaly, Cu \geq 27.8ppm
 - Soil Anomaly, Cu \geq 50.0ppm
 - Soil Anomaly, Cu \geq 70.1ppm
 - Soil Anomaly, Cu \geq 100.0ppm
 - Soil Anomaly, Cu \geq 177.1ppm
- Phase I Geochemical Survey
- Soil Anomaly, Cu \geq 73.3ppm
 - Soil Anomaly, PC \geq 0.74
 - Soil Anomaly, Cu \geq 73.3ppm & PC \geq 0.74

250 0 250 500 750 1000 1250
(meters)

JICA - MMAJ
Pringani, Inyati,
Lions den area
Summary of Analyses
of previous
geochemical survey
DOXA Engineering Co., LTD. 1993

Fig.II-1-4 Summary of the analyses of previous geochemical survey (Pringani, Inyati, Lions den area)

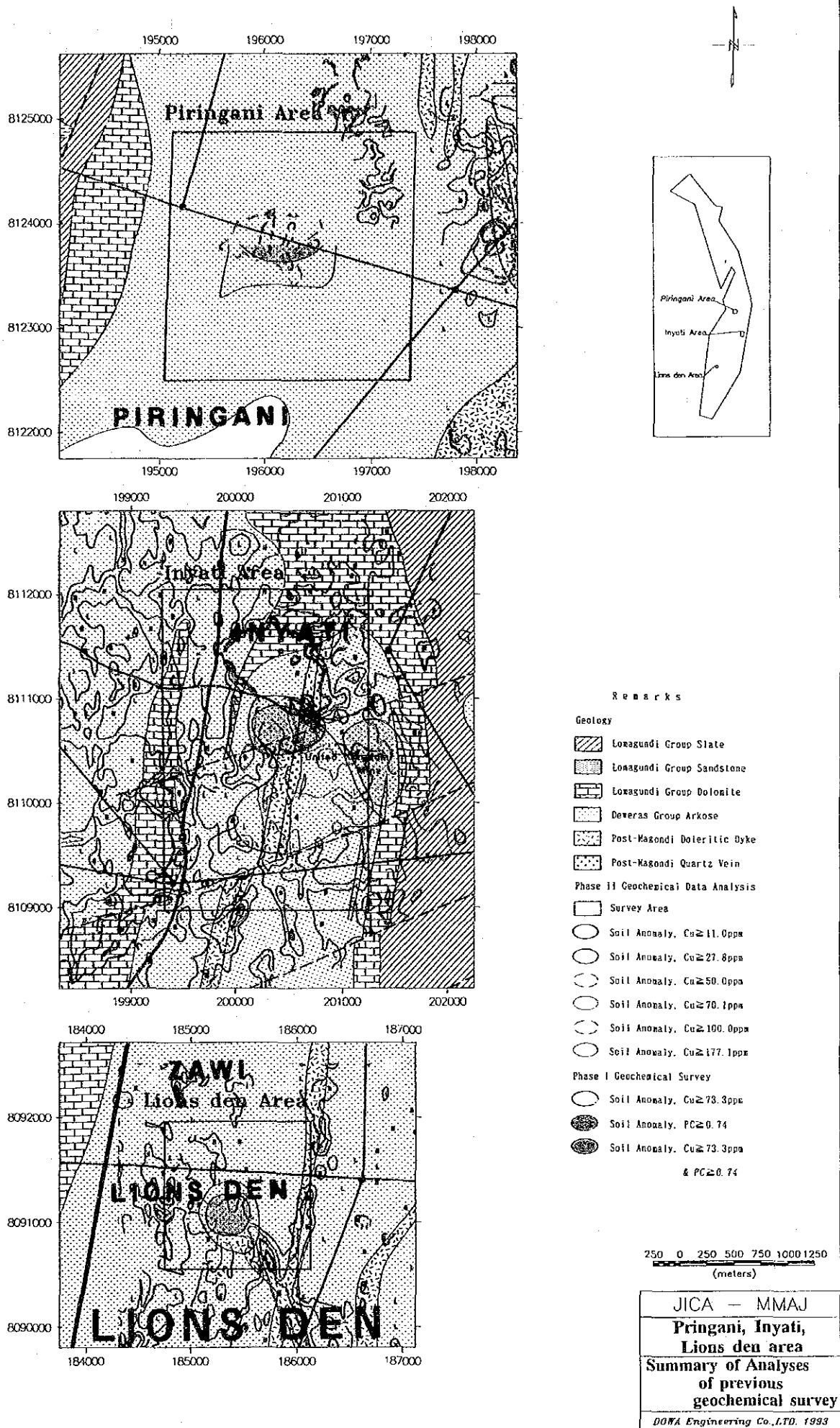


Fig.II-1-4 Summary of the analyses of previous geochemical survey (Pringani, Inyati, Lions den area)

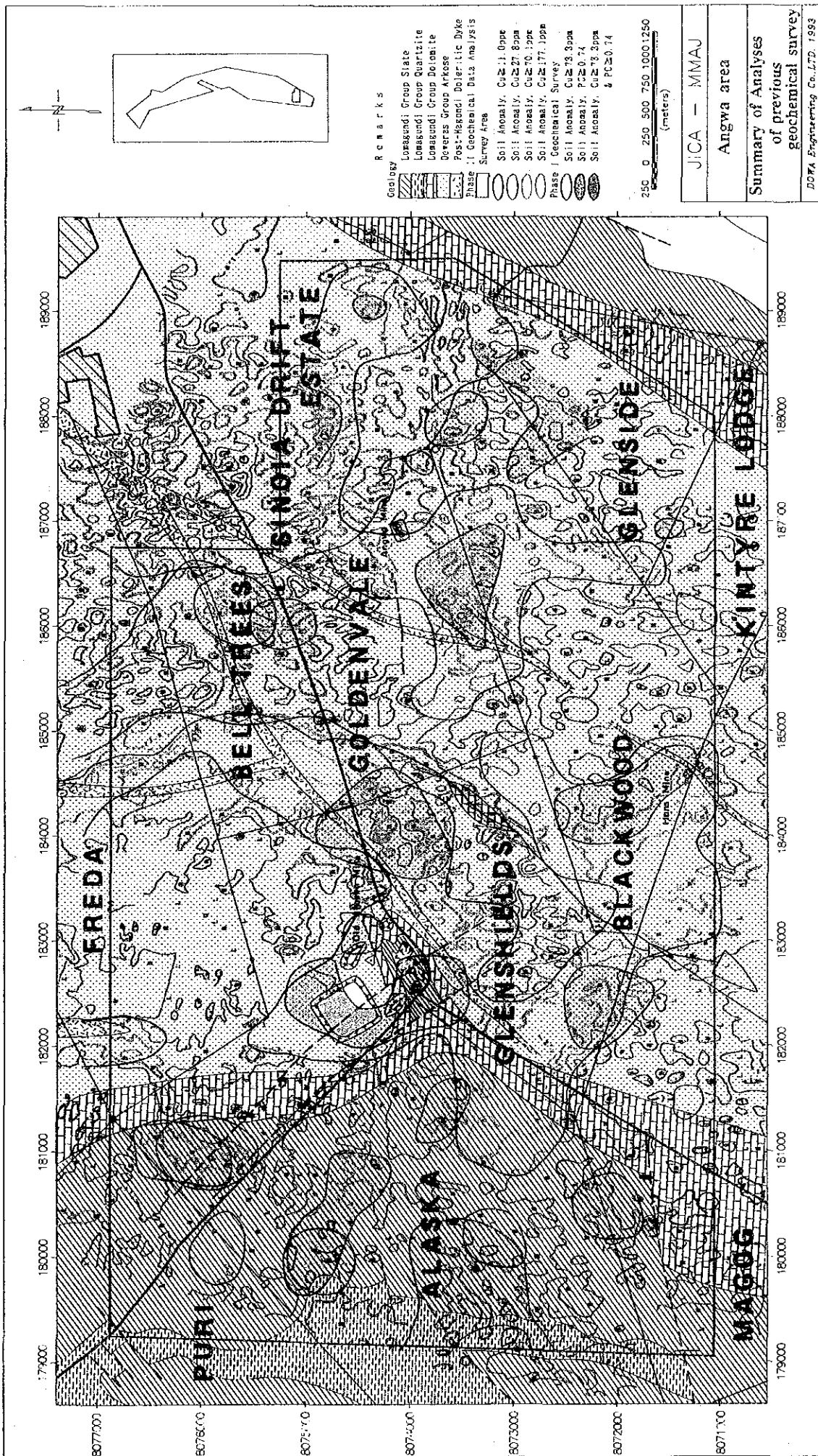
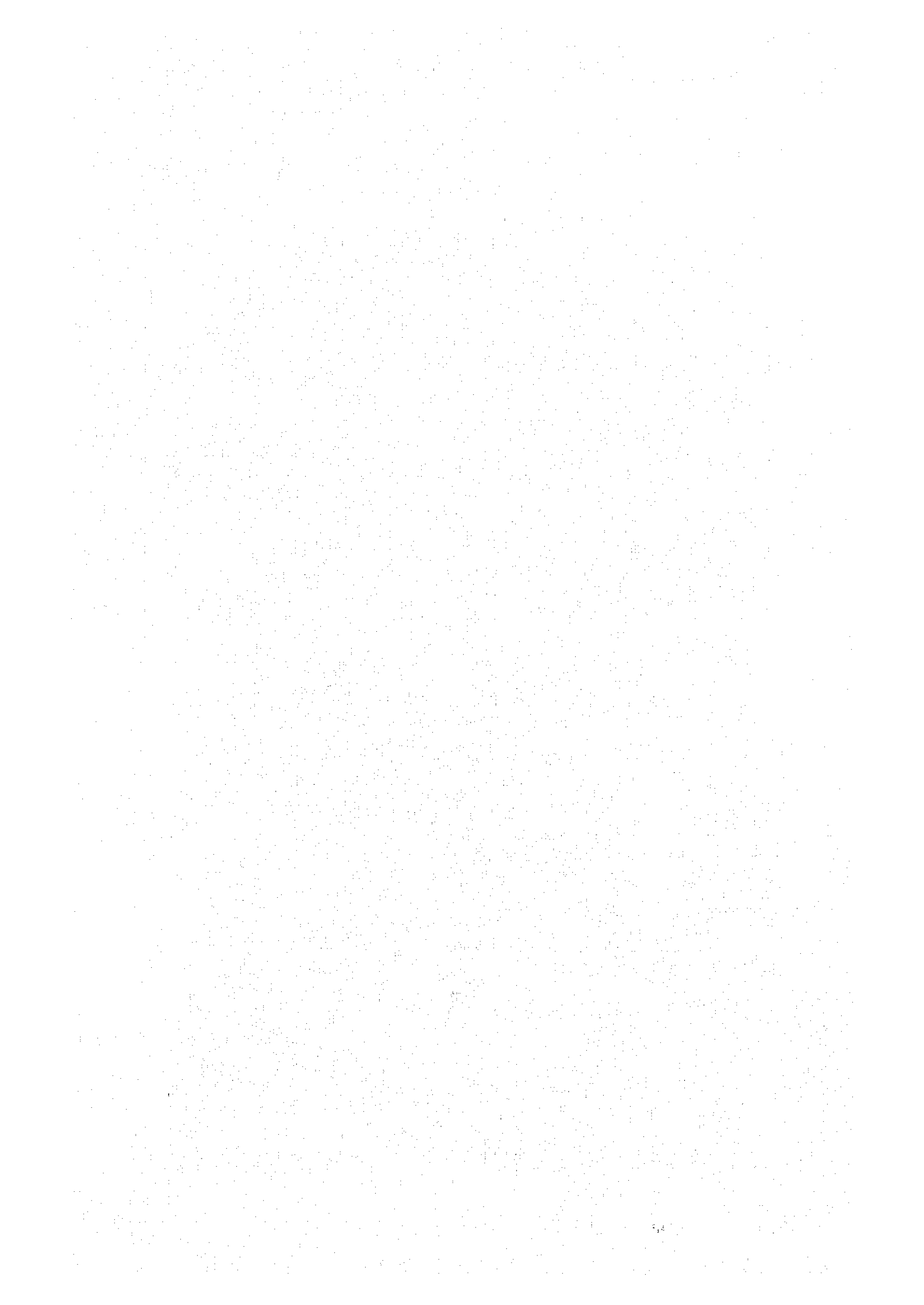


Fig.II-1-4 Summary of the analyses of previous geochemical survey (Angwa area)



Chapter 2. Geophysical survey

2-1. Method of the survey

2-1-1. Contents of the survey

Geophysical electrical methods of prospecting were carried out using IP method in two stages. One was to set up the survey lines on the geochemical anomalous places as reconnaissance. The other was to set up new survey lines parallel to the IP anomalous zones and setting up extension survey lines as a semi-detailed survey.

Specifications of the geophysical survey are shown in Table II-2-1. The index map of the survey area is shown in Fig.I-1-1.

TableII-2-1 Specification of the geophysical survey

| | reconnaissance survey | semi-detailed survey |
|---|--|----------------------|
| method | Induced polarisation method(IP method) | |
| detection method | Time domain method | |
| electrode arrangements | dipole-dipole arrangement | |
| Separation of electrodes | a=200m | a=200m, a=100m |
| Coefficient of separation of electrode | n=1 ~ 4 | |
| number of survey lines | 21 | 12 |
| Total length of survey lines | 51.0km | 23.2km |
| Measurement of physical properties(laboratory test) of rocks and ores | chargeability and resistivity 60 specimens | |

2-1-2. Operation

1. Determination of survey lines and survey

After plotting the locations of Cu anomalous places(positioning by GPS) on the map, the lines were determined from the starting point, which was decided as the suitable point with bench mark such as crossing of road, river or power cable. The direction of the lines were decided to be at right angles to the strike of geology. The survey was carried out using pocket compass and esron tape.

The lines are shown in Fig.II-2-1.

2. Electric survey (IP method)

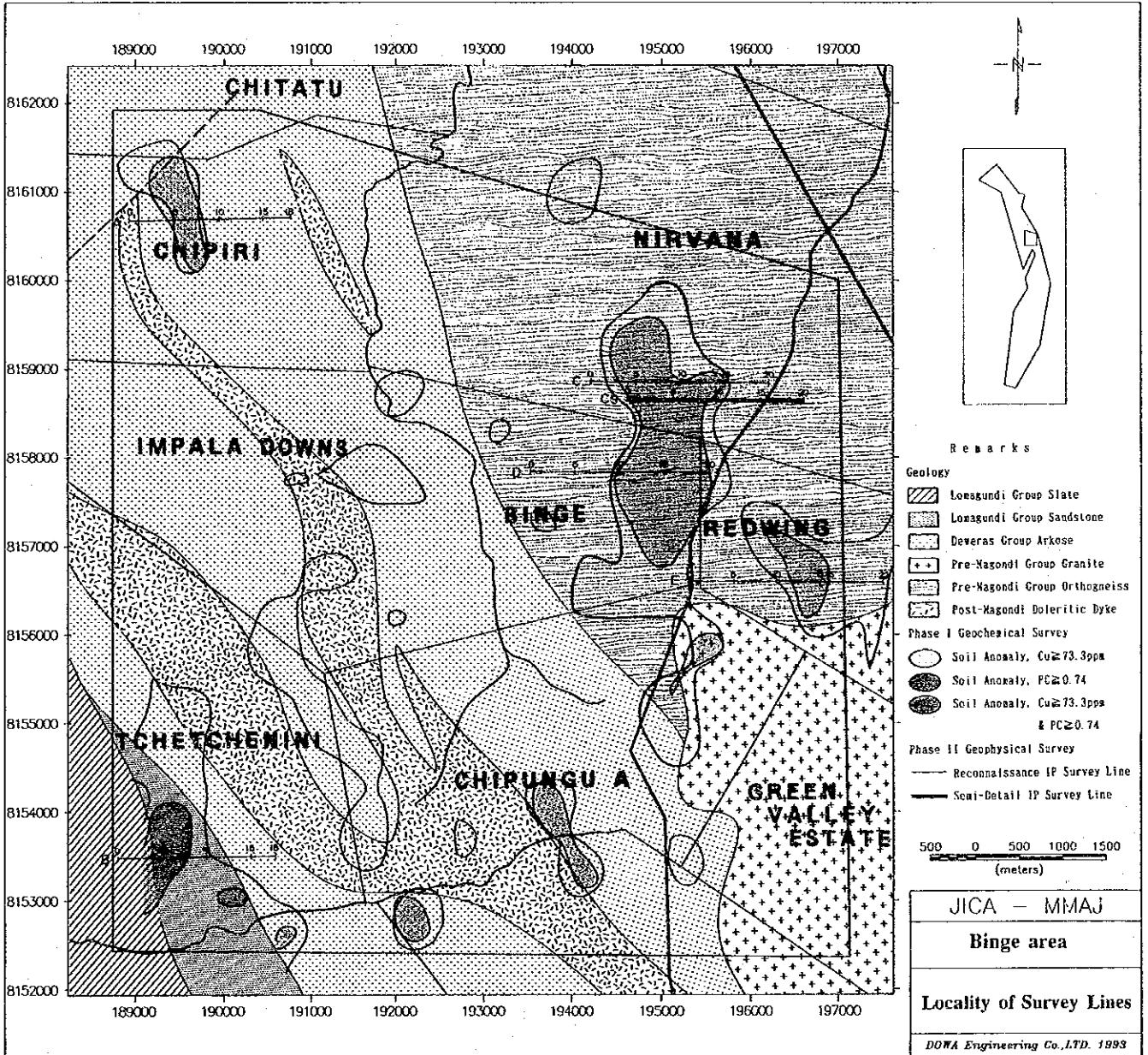


Fig.II-2-1 Locality of Survey Lines (Binge area)

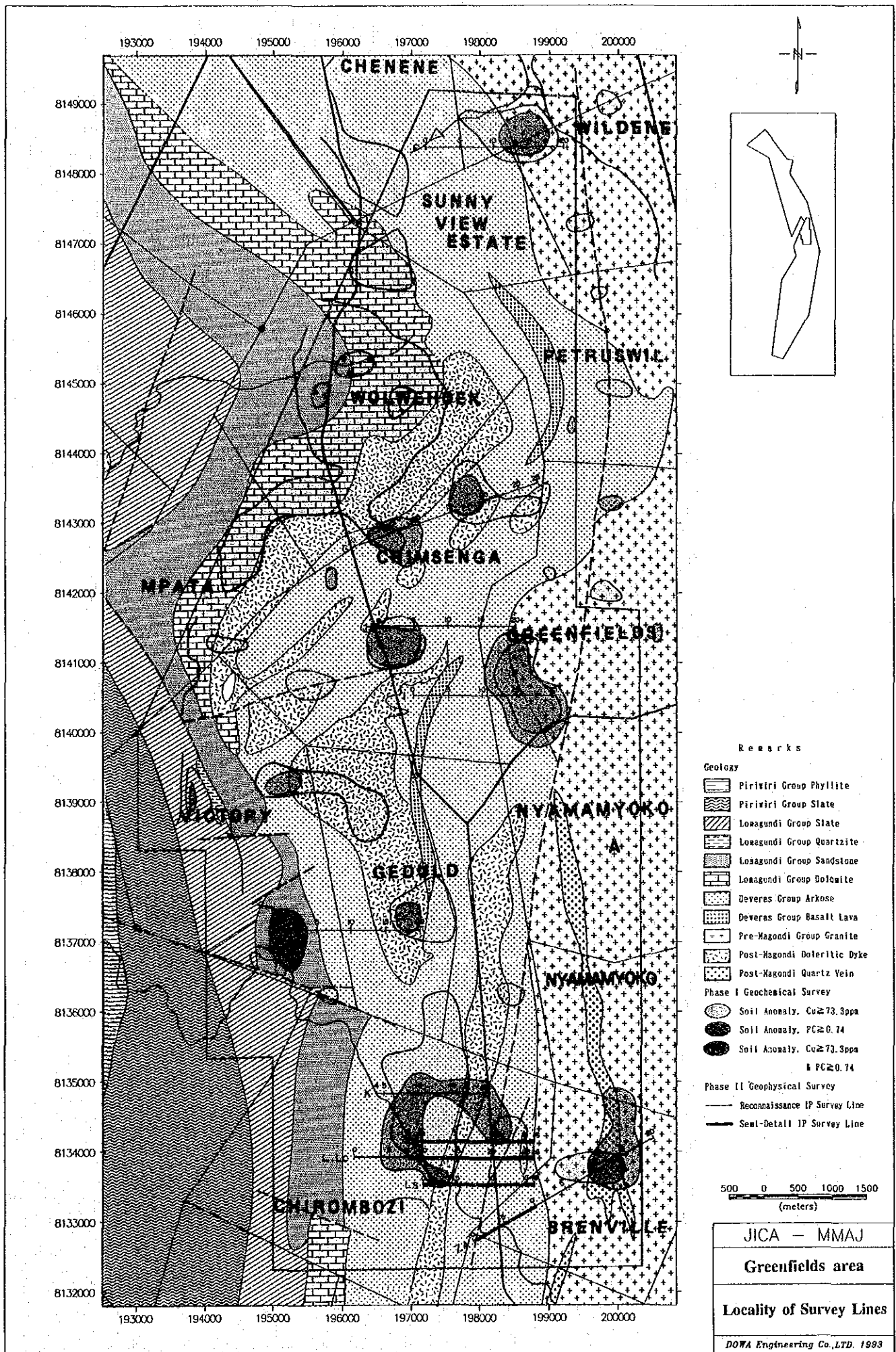


Fig.II-2-1 Locality of Survey Lines (Greenfields area)

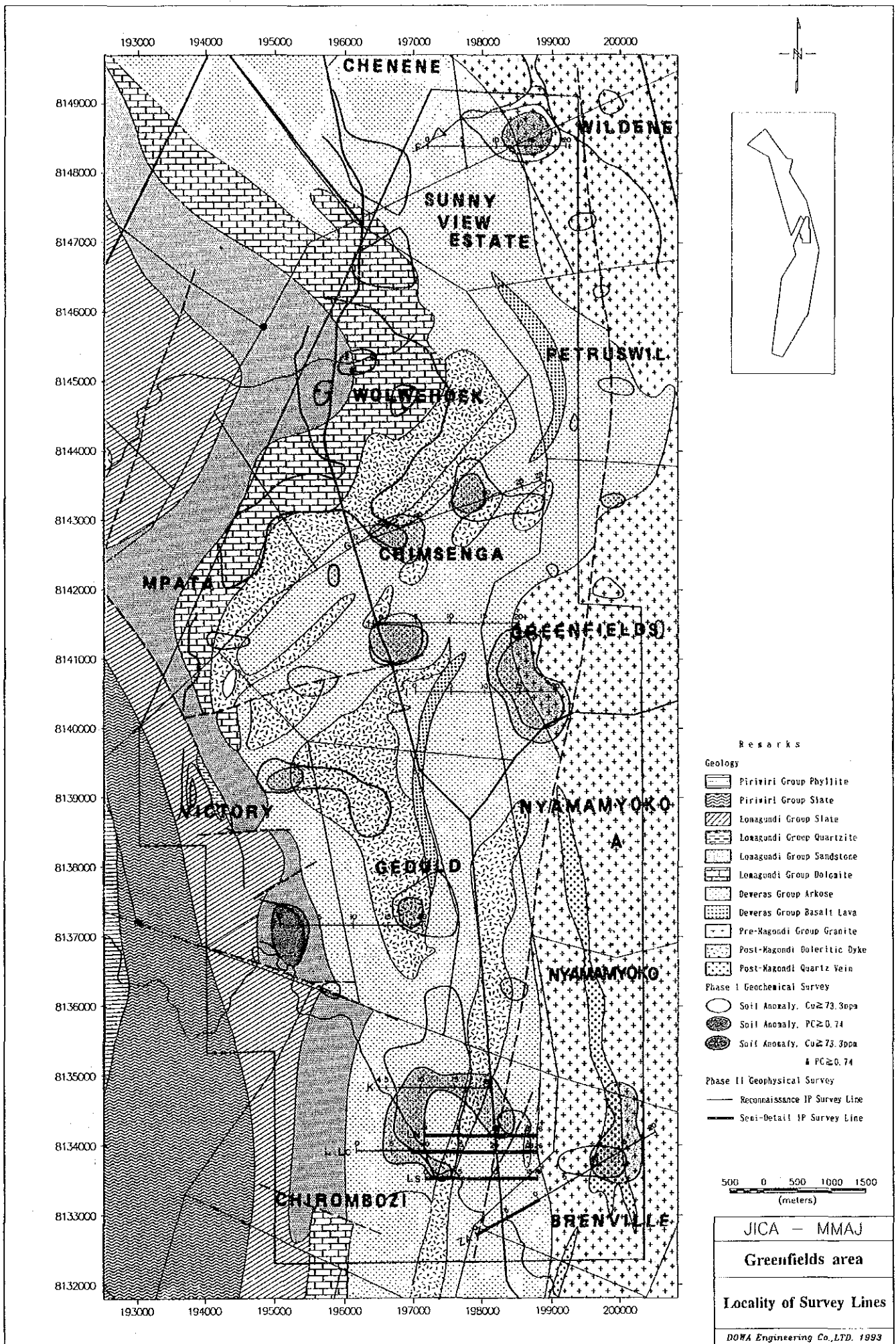
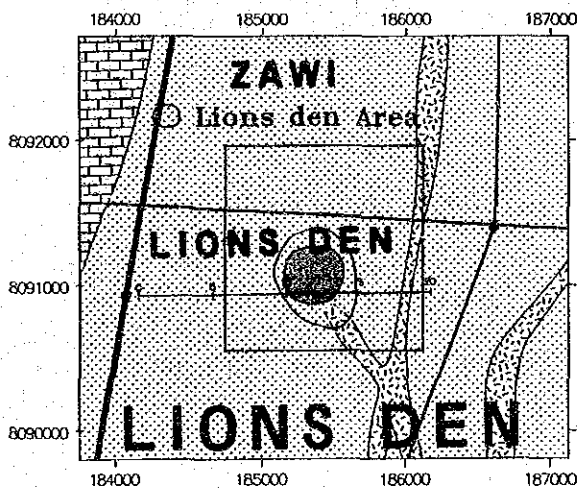
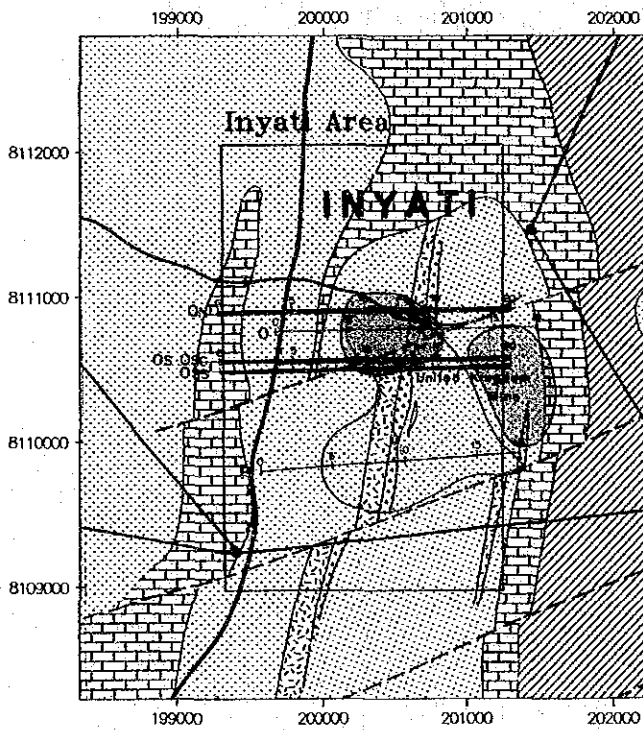
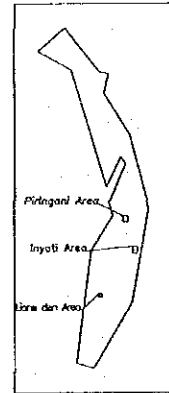
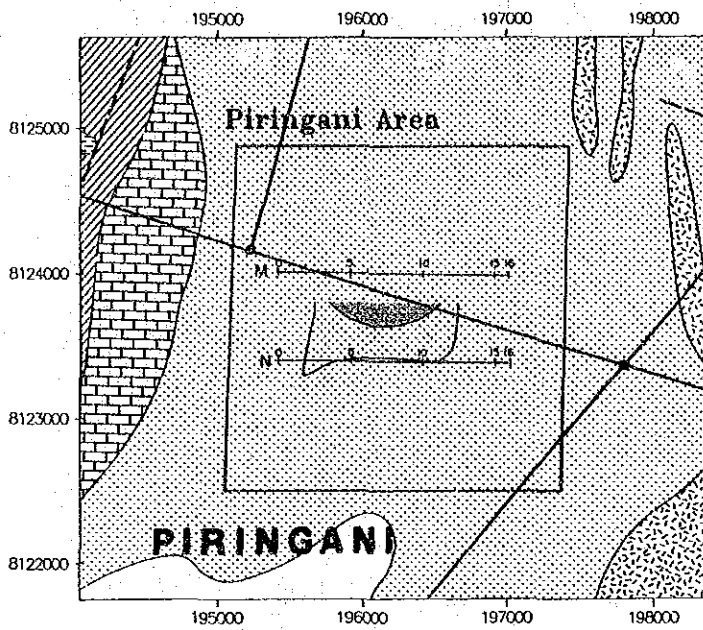


Fig.II-2-1 Locality of Survey Lines (Greenfields area)



Remarks

Geology

- Lonagundi Group Slate
- Lonagundi Group Sandstone
- Lonagundi Group Dolomite
- Deveras Group Arkose
- Post-Magondi Doleritic Dyke
- Post-Magondi Quartz Vein

Phase I Geochemical Survey

- Soil Anomaly, $Cu \geq 73.3ppm$
- Soil Anomaly, $PC \geq 0.74$
- Soil Anomaly, $Cu \geq 73.3ppm$ & $PC \geq 0.74$

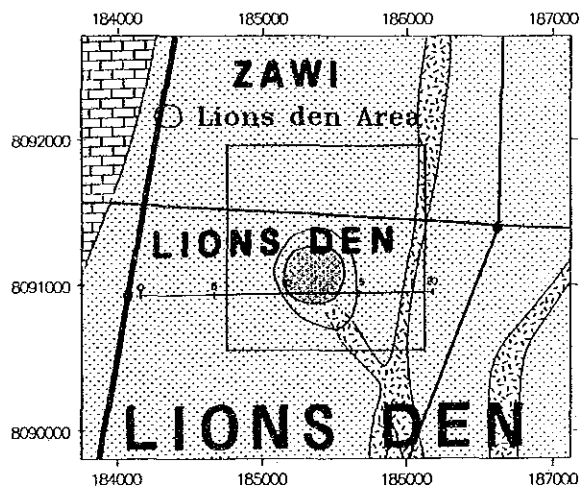
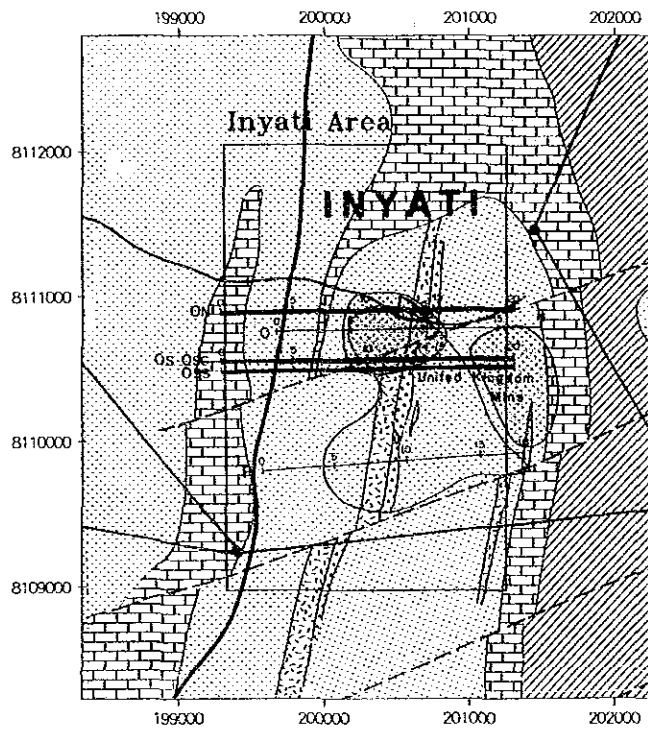
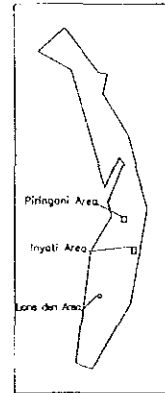
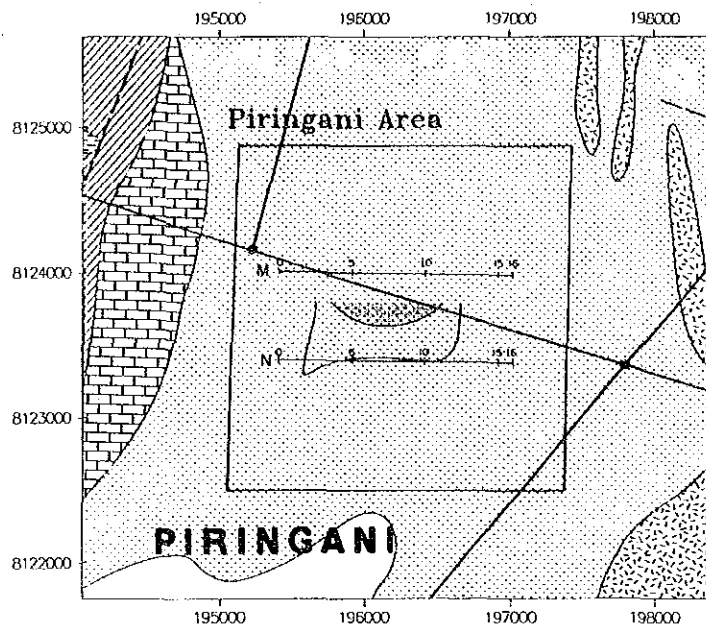
Phase II Geophysical Survey

- Reconnaissance IP Survey Line
- Semi-Detail IP Survey Line

250 0 250 500 750 1000 1250
(meters)

| |
|-------------------------------------|
| JICA - MMAJ |
| Pringani, Inyati, Lions den area |
| Locality of Survey Lines |
| DOWA Engineering Co., LTD. 1999 |

Fig.II-2-1 Locality of Survey Lines (Pringani, Inyati, Lions den area)



- Remarks
- Geology
- Lonagundi Group Slate
 - Lonagundi Group Sandstone
 - Lonagundi Group Dolomite
 - Deveras Group Arkose
 - Post-Magondi Doleritic Dyke
 - Post-Magondi Quartz Vein
- Phase I Geochemical Survey
- Soil Anomaly, Cu \geq 73.3ppm
 - Soil Anomaly, PC \geq 0.74
 - Soil Anomaly, Cu \geq 73.3ppm & PC \geq 0.74
- Phase II Geophysical Survey
- Reconnaissance IP Survey Line
 - Semi-Detail IP Survey Line

250 0 250 500 750 1000 1250
(meters)

JICA - MMAJ
Pringani, Inyati,
Lions den area
Locality of Survey Lines
DOWA Engineering Co., LTD. 1993

Fig.II-2-1 Locality of Survey Lines (Pringani, Inyati, Lions den area)

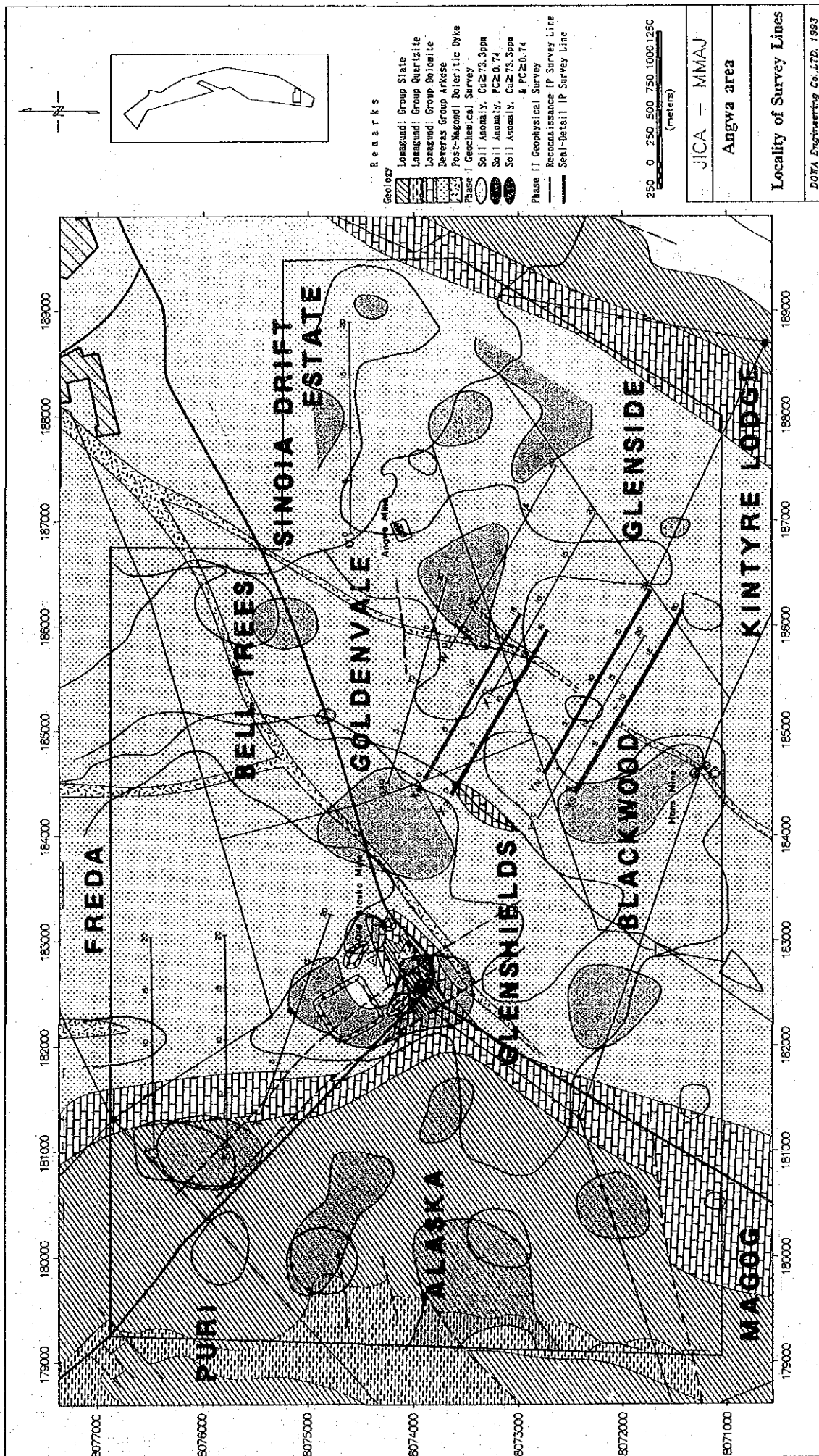


Fig.II-2-1 Locality of Survey Lines (Angwa area)

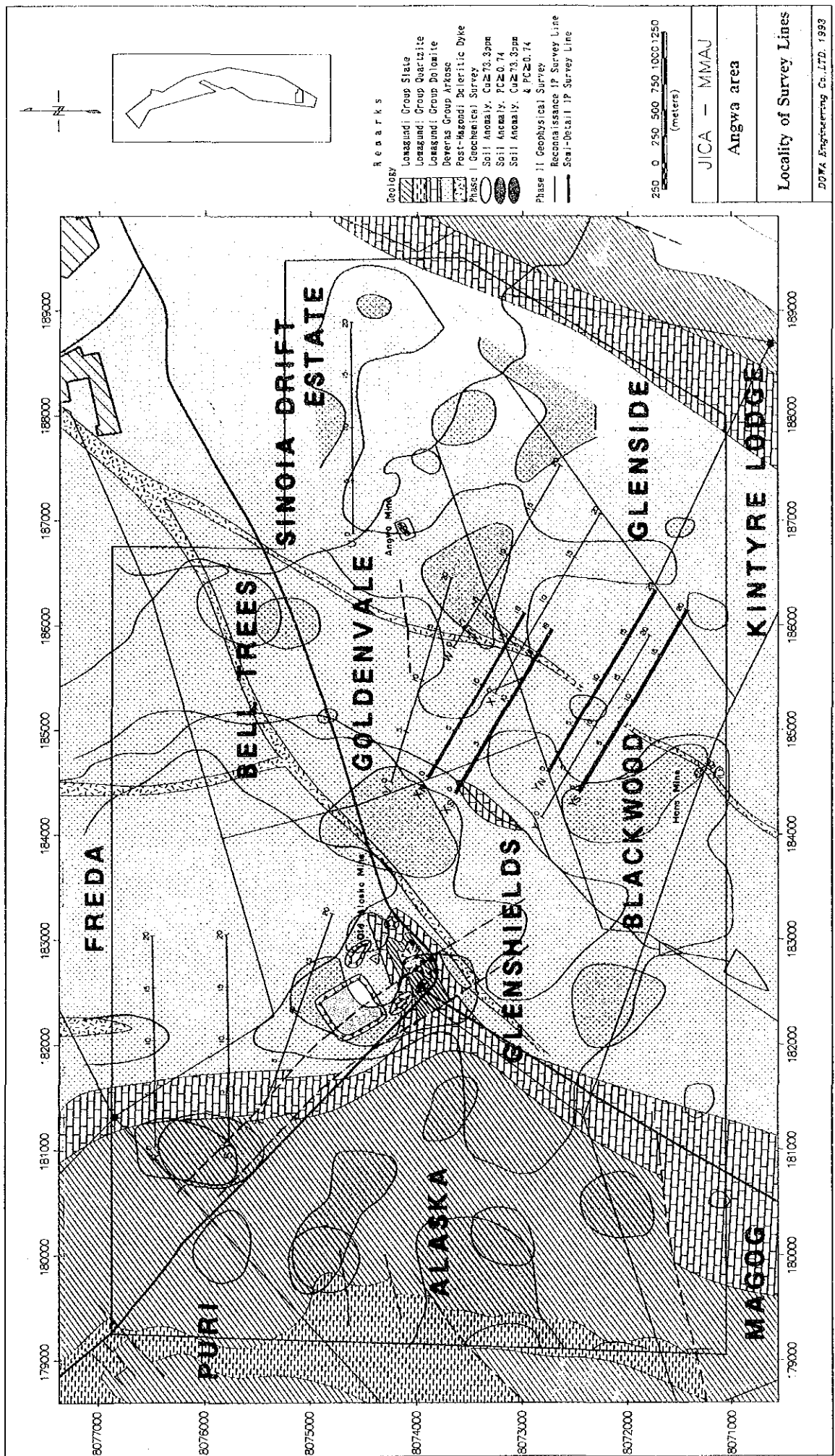
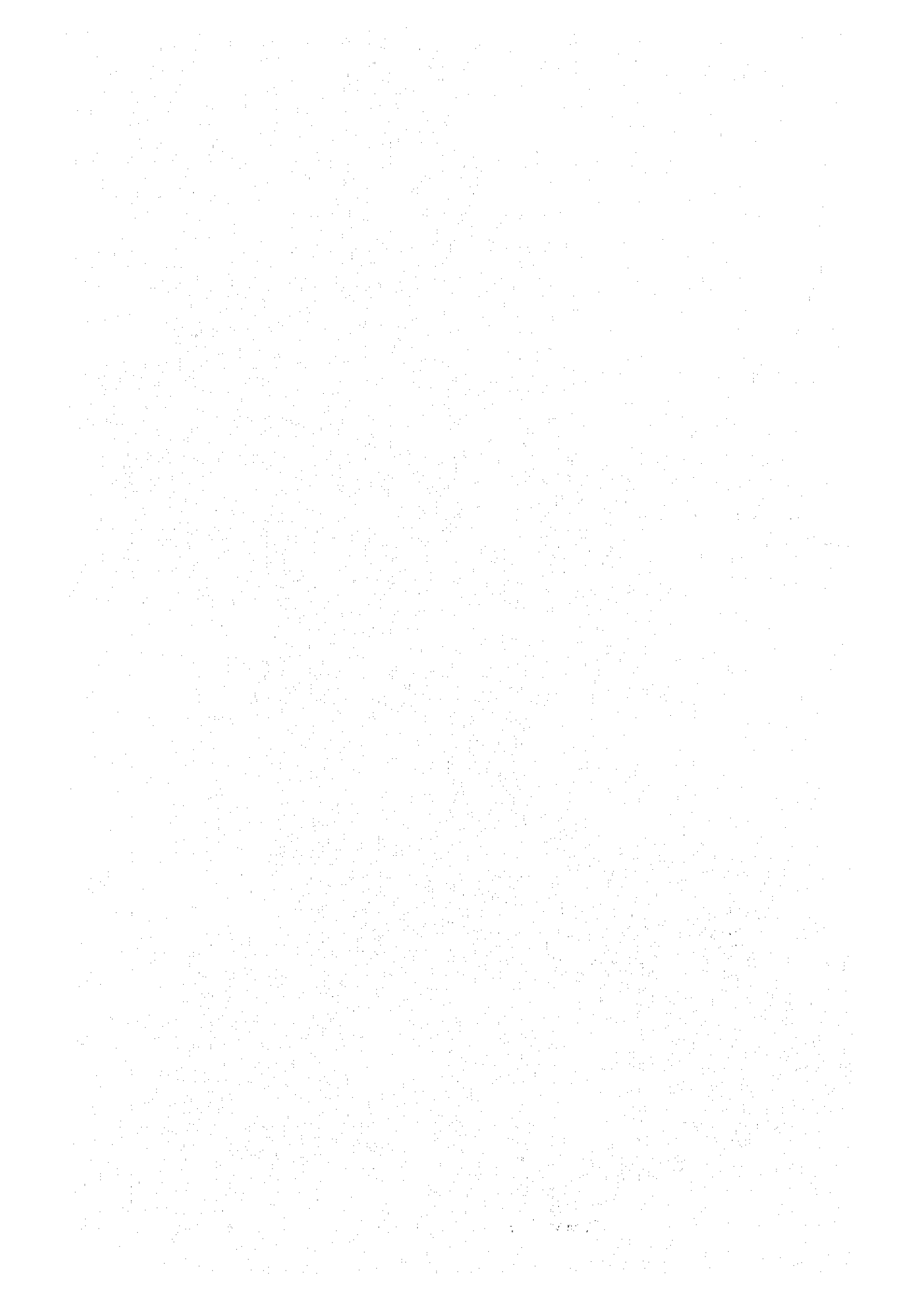


Fig.II-2-1 Locality of Survey Lines (Angwa area)



1) Principles of IP method

Electro-chemical phenomena occurs by current introduction into the earth. The following two phenomena are measured by IP method:

[Over Voltage Effect]

Two electrical layers are introduction in sulphide and metal conductors by turning the electrical power. This phenomenon is the complex effect of ion and electron conduction. This phenomenon can be observed in the minerals with electron conductivity. This phenomenon is the observation target of IP method.

[Normal Effect or Background]

Polarisation occurs in ordinary rocks by current introduction. This phenomenon is caused by membrane polarisation of clay minerals. The membrane polarisation of montmorillonite is biggest and the polarisation of kaolinite is small in various clay minerals. The membrane polarisation shows maximum, when there is 5% capacity ratio of clay minerals, however, the polarisation decreases also by 5% ratio.

The maximum value of the membrane polarisation is approximately 2% in Fc value when the capacity ratio of montmorillonite is 5%. This value is very small compared to Over Voltage Effect of sulphide minerals.

2) Measuring method of IP phenomena

The outline of measurement is shown in Fig.II-2-2.

The measurement was carried out by the time-domain method. A couple of current electrodes and another couple of potential electrode are used in the time-domain method. The intermittent electric current (on/off 2.0sec) was introduced into the earth through the current electrodes, and the primary potential difference(V_p) just before switching off the power and the secondary potential difference(V_s) just after was switching off the power is measured between another couple of potential electrodes.

V_s was measured in the time t (4msec ~ 14msec) after the power was switched off in this survey.

The measured values of IP effect by IP method is called chargeability. They are shown as $V_s(t_n)/V_p$ [mV/V].

The secondary potential difference of this survey shows high resistivity of this area, and the effect of coupling of electro-magnetism was hardly shown. Wide-point 935 msec data of chargeability was selected for chargeability distribution map.

The concept of operation is shown in Fig.II-2-2. The concept of the method of measurement is shown in Fig.II-2-3 and the list of sampling time is shown Table in II-2-2.

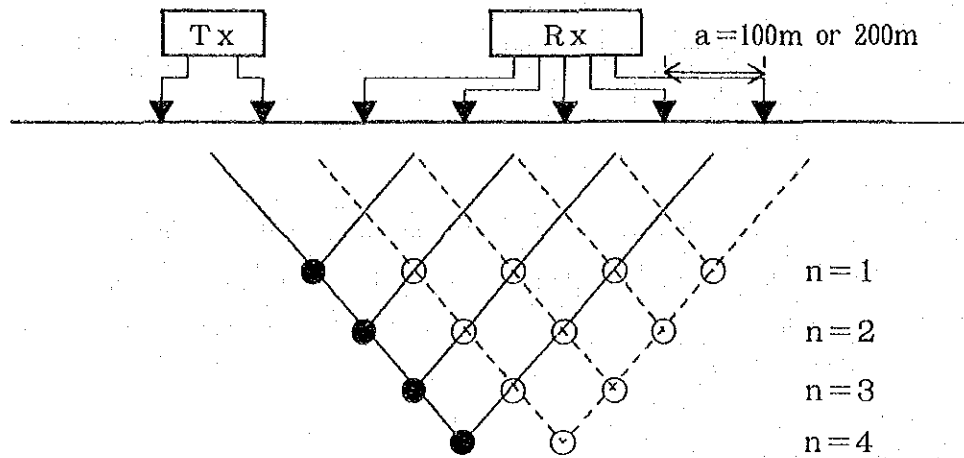


Fig.II-2-2 Concept of operation

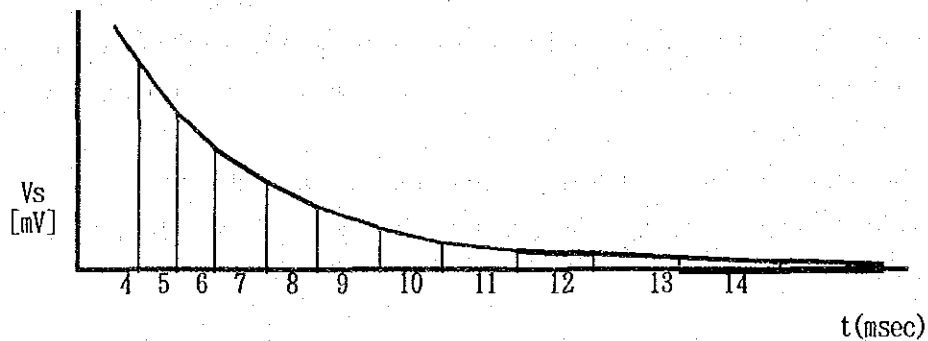


Fig.II-2-3 Concept of method of measurement

TableII-2-2 List of the sampling time

| Slice # | 4 | 5 | 6 | 7 | 8 | 9 | 10 | 11 | 12 | 13 | 14 |
|---------------|----|----|-----|-----|-----|-----|-----|-----|-----|------|------|
| Width (msec) | 20 | 40 | 40 | 80 | 80 | 140 | 140 | 230 | 230 | 360 | 360 |
| Mid-Point (") | 60 | 90 | 130 | 190 | 270 | 380 | 520 | 705 | 935 | 1230 | 1590 |

3. Measurement of the physical properties of the rocks

IP measurements of 60 specimens of representative rocks and ores of this area were carried out in order to collect the fundamental data of the electrical characteristics of the rocks.

IP and resistivity measurements were carried out by the time-domain method after cutting four surfaces of each rock and dipping in tap water for a period of 1 day. The same receiver used in field was used in the this measurement.

4. Measuring equipments and materials

The measuring equipments and materials are shown in Table II-2-3.

TableII-2-3 List of equipments and materials

(field survey)

| equipment | maker | type | specification | amount |
|-------------------------|----------|--|--|--------|
| Transmitter | IRIS | ELECTRA V/I 1000 | 1000V,4A max output:1000W | 1 |
| Engine Generator | KUBOTA | AE2200 | 50Hz 220V 1.9KVA single cylinder 4cycle | 1 |
| Receiver | SCINTREX | IPR-12 | 8channel,14window Input Range:50μV to 14V | 1 |
| Electrode | | current electrode potential electrode | copper (gauze) CuSO ₄ | 1 |
| cable | Fujikura | | VSF1.25mm ² cable,co-axial cable | 1 |
| measuring compass | Ushikata | pocket compass | 100m Esron tape | 4 4 |
| communication device | sony | ICB-88H | output:500mW | 12 |

(Laboratory test)

| | | | | |
|-------------|----------|--------|---|---|
| Transmitter | IRIS | IP-L | output:1μA ~ 100μA max 10V | 1 |
| Receiver | SCINTREX | IPR-12 | 8channel,14window Input Range:50μV ~ 14V | 1 |
| electrode | | Pt | | 1 |

2-1-3. Data Processing

Simulation analysis of provisional section.

The electric field due to the point of origin of current of the earth's surface and/or underground, distributes minimum energy potentiality. In this case, the condition of the energy of the electric field is shown in the following partial differential equation.

$$\Delta f \nabla f(\phi) dV = 0 \quad (1)$$

In this equation $f(\phi)$ is the function introduced from the electro-magnetic equation of Maxwell. It is shown in the following equation using conductivity Ω and current density J_s when the electric field is constant.

$$f(\phi) = \sigma(\Delta f)^2 - 2J_s \cdot \Delta f \quad (2)$$

Equation (1) is the integration for the cubic content of the ground in which current is introduced. Approximation by finite element method is carried out using the limited cubic content with enough volume. The analysis of this survey was carried out as a two dimensional problem, because the cross section with enough width(10km in horizontal × 3km in vertical) was chosen instead of cubic content.

The simulation analyses of resistivity and IP suspected section was carried out by 2.5 dimensional finite element method programs of Coggon(1971) and Rijo(1977). In these analyses, several ten times of repetition was made by conversational mode of model input and amendment until the completion of approximation to suspected section.

2-2. Results of survey

2-2-1. Pre-survey

Pre-survey above the existing ore deposit(the Avondale deposit) was carried out in order to study IP effect of this area before the reconnaissance. Geology, resistivity and vertical distribution of IP of the Avondale ore deposit is shown in Fig.II-2-4. Very low resistivity(150 to 400 $\Omega\cdot m$) is observed in electrodes separation $a=100m$ and $200m$.

Obvious IP anomaly by comparatively shallow IP anomalous body is observed on the stations No.6 to 7 in both the electrodes separation. It corresponds well to the distribution of the ore deposit.

2-2-2. Result of reconnaissance

1. Apparent resistivities and IP section of the reconnaissance survey

Sections of apparent resistivities and IP of the reconnaissance survey are, shown in Fig.II-2-5 Fig.II-2-6.

The Binge site(Fig.II-2-5(1), Fig.II-6-1(1))

A line

Arkose of the Deweras group is distributed.

Resistivity shows approximately 700 $\Omega\cdot m$ in the eastern side of station No.6, but it generally shows high resistivity more than 1,000 $\Omega\cdot m$.

Maximum Ip shows 6.1mV and no peculiar IP pattern is recognised.

B line

Slate and sandstone of the Lomagundi group, and arkose of the Deweras group are distributed from the west.

Resistivity shows 64~1,400 $\Omega\cdot m$, and is generally low less than 700 $\Omega\cdot m$.

Low resistivity zones(less than 100 $\Omega\cdot m$) from the station No.0 to No.4 corresponds to slate.

Resistivity of the stations No.5 to No.12 is 100 to 400 $\Omega\cdot m$, which corresponds to sandstone.

Resistivity of the eastern part is more than 700 $\Omega\cdot m$, which corresponds to arkose.

Obvious IP anomaly(maximum 9.6mV) is recognised on the stations No.2 to No.12.

IP anomalies are recognised corresponding to slate, sandstone and arkose.

C line

The Pre-Magondi gneiss is distributed.

Resistivity shows 300 to 3,000 Ω -m approximately, low resistivity is shown in centre part of the line.

Low resistivity/low IP and high resistivity(approximate 3,000 Ω -m)/high IP(maximum 8.2mV/V) are shown to be coupled.

IP anomalies of the deep part below the stations of No.4 and No.12 to No.14 are obvious.

D line

The pre-Magondi gneiss is distributed.

Resistivity shows 87 to 2,800 Ω -m.

The anomalies of low resistivity(120 Ω -m)/high IP(maximum 8.8mV/V) are recognised just at the stations No.6 and No.10 to 14, however indistinct IP patterns are shown.

E line

The Pre-Magondi gneiss is distributed.

Resistivity shows 130 to 3,100 Ω -m.

Low resistivity/low IP and high resistivity/high IP are the general tendency, but IP shows low value of maximum 5.0mV/V.

The Greenfields site (Fig.II-2-5(2)-(3).Fig.II-2-6(2)-(3))

F line

Granite of the Pre-Magondi intrusives and arkose of the Deweras group distributed in the eastern part and western part respectively.

Resistivity shows 420 ~ 3,100 Ω -m.

The high resistivity zones whose values are more than 1,500 Ω -m cover almost all the area. The high resistivity area does not correspond to the geology.

No characteristics are recognised in the low IP(less than 5.6mV/V) distribution areas.

G line

Arkose and small scale doleritic intrusives are distributed.

Resistivity shows 196 ~ 1,000 Ω -m.

Low resistivity(less than 700 Ω -m)/low IP(less than 6mV/V) is the general tendency.

No characteristics are recognised in the IP anomaly distribution.

H line

Arkose of the Deweras group is distributed.

Resistivity shows 150 ~ 580 Ω -m.

Low resistivity(less than 300 Ω -m)/low IP(4.9mV/V in maximum) is the general tendency.

No characteristics are recognised in the IP anomaly distribution.

I line

The basement granite and arkose are distributed, respectively, in the eastern part and western part.

Resistivity shows 250 ~ 4,200 Ω ·m.

High resistivity zone in the eastern part corresponds to granite and low resistivity zone (approximate 400 Ω ·m) corresponds to arkose.

The general tendency is low IP distribution, but, slightly high IP (7.7mV/V) is shown in the western shallow part.

J line

Arkose occurs in the eastern part, basic intrusives and sandstone occur in the western part.

Resistivity shows 240 ~ 830 Ω ·m.

Low resistivity (less than approximate 700 Ω ·m)/low IP (less than 4.5mV/V) is the general tendency.

K line

Arkose of the Deweras group is distributed with basic intrusives in the eastern part of the survey line.

Low resistivity (less than 600 Ω ·m)/low IP (less than 5mV/V) is generally shown.

L line

Arkose of the Deweras group is distributed with basic intrusives in the central part of the survey line.

Resistivity shows less than 175 ~ 1,100 Ω ·m.

IP value of the eastern part of the stations No.14 to No.20 shows a high value (10.6mV/V) and it forms a part of IP anomaly.

Za line

The basement granite in the eastern part and arkose of the Deweras group in the western part are distributed, respectively.

Resistivity of the western margin (600 Ω ·m) and the value more than 1,500 Ω ·m is shown in other area.

A part of the obvious IP anomaly (9mV/V) is detected. The IP anomaly nearly corresponds to the boundary area of arkose and granite.

The Piringani site (Fig.II-2-5(3), Fig.II-2-6(3))

This site is located in the distribution area of arkose of the Deweras group.

M line

Resistivity shows 92 ~ 720 Ω ·m.

Low resistivity(300 Ω ·m)/low IP(5mV/V) is the general tendency.

A weak IP anomalous pattern is recognised in the shallow part of station No.6.

N line

Resistivity 140 ~ 500 Ω ·m.

Low resistivity(300 Ω ·m)/low IP distribution is generally shown.

Weak IP anomalous patterns by the shallow IP anomalous body are recognised on the stations No.6 to No.14.

The Inyati site(Fig.II-2-5(4),Fig.II-2-6(4))

Arkose of the Deweras group, doleritic dykes and Quartz-calcite veins are distributed.

O line

Resistivity shows 170 ~ 1,400 Ω ·m.

Resistivity is generally less than 700 Ω ·m.

Comparatively distinct IP anomalous patterns are shown on station No.6 to No.8 caused by the shallow anomalous body.

The IP anomalous body corresponds to the quartz-calcite veins area.

P line

Resistivity shows 150 ~ 2,600 Ω ·m.

No characteristics were recognised in the IP anomalous pattern.

The Lions Den site(Fig.II-2-5(4), Fig.II-2-5(4))

Arkose of the Deweras group and doleritic dykes are distributed.

Q line

Resistivity is less than approximately 700 Ω ·m.

Comparatively distinct IP anomalous pattern by the shallow IP anomalous body is shown near station No.6 to No.8, however, the IP anomaly is low(6.6mV/V in maximum).

The Angwa site(Fig.II-2-5(4)-(5), Fig.II-2-6(4)-(5))

Arkose of the Deweras group is widely distributed. Dolomite and slate of the Lomagundi group are distributed in the western part.

R line

The stations No.0 to 2, No.2 to No.7 and No.7 to No.20 correspond to slate, dolomite and arkose, respectively.

Resistivity shows $170 \sim 1,200\Omega\cdot\text{m}$.

Slightly high IP(5.8mV/V) is shown near the surface of the stations No.0 to No.2 and the deep part of the stations No.6 to No.8. The IP anomaly of the shallow part of the stations of No.0 to No.2 and the IP anomaly of the deep part are recognised in slate area and the boundary area of dolomite and arkose.

S line

Geology is almost the same as R line

The IP pattern resembles that of R line.

IP anomaly in the deep part of the station No.6 to No.8 is indistinctly enlarged.

T line

Resistivity shows $220 \sim 1,500\Omega\cdot\text{m}$.

The western end and the eastern end of the lines correspond to dolomite and arkose, respectively. However, the correspondence between resistivity and lithology is not recognised.

Low resistivity/low IP is shown, and no peculiar IP pattern is recognised.

U line

Resistivity shows $220 \sim 1,500\Omega\cdot\text{m}$.

The low resistivity zone of the western shallow part corresponds to arkose.

Low resistivity/low IP is shown and no peculiar IP pattern is recognised.

Slightly high IP(5.5mV/V) is shown in the western end of the line.

V line

The geology comprise basic dykes in the distribution area of arkose.

Resistivity shows $410 \sim 2,700\Omega\cdot\text{m}$.

Slightly low IP(6.0mV/V) is shown on the stations of NO.6 to No.20. However, the IP pattern is generally indistinct.

W line

The geology comprise basic dykes in the distribution area of arkose.

Resistivity shows $145 \sim 1,500\Omega\cdot\text{m}$.

Slightly low IP(6.3mV/V) is shown in the shallow part of the stations No.4 to No.6.

Slightly high IP(6.0mV/V) is shown in the deep part of the No.12 station.

X line

The geology comprise basic dykes in the distribution area of arkose.

Resistivity shows 220 ~ 1,600 Ω ·m.

High resistivity(1,600 Ω ·m)/high IP(8.8mV/V) are shown in the eastern and the western part of the line.

Y line

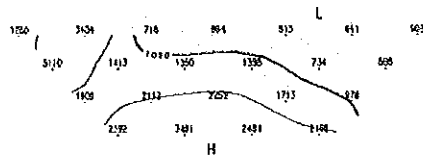
The geology comprise basic dyke in the distribution area of arkose.

High resistivity/high IP(9.6mV/V) are generally shown.

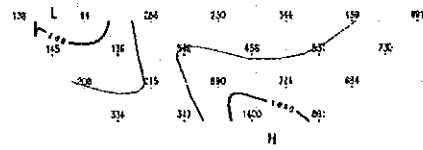
Resistivity shows 370 ~ 2,300 Ω ·m.

The distinct IP anomaly is recognised on the stations of No.16 to No.18. The characteristics of resistivity and IP distribution of each line are summarised from the results above and are shown in Table.II-2-4.

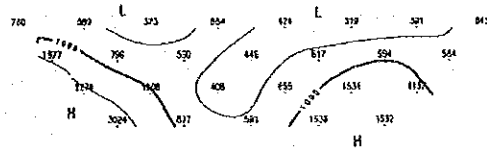
LINE-A 0 2 4 6 8 10 12 14 16 18



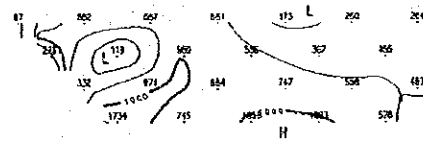
LINE-B 0 2 4 6 8 10 12 14 16 18



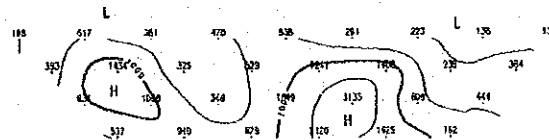
LINE-C 0 2 4 6 8 10 12 14 16 18 20



LINE-D 0 2 4 6 8 10 12 14 16 18 20



LINE-E 0 2 4 6 8 10 12 14 16 18 20 22



100 0 100 200 300 400 500
(meters)

UNIT: ($\Omega \cdot m$)

Fig.II-2-5(1) Section of apparent resistivity of the reconnaissance

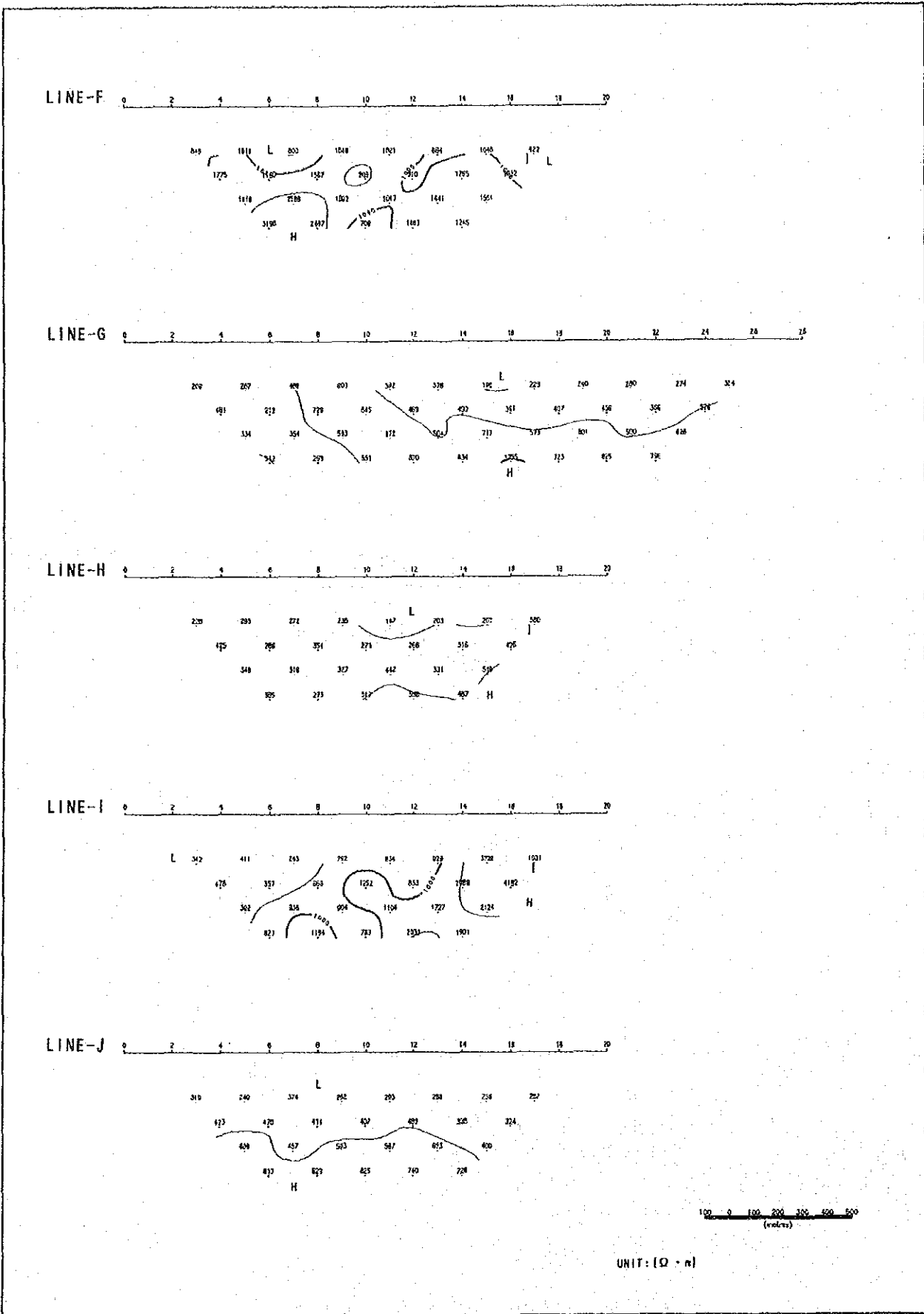
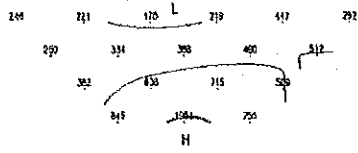
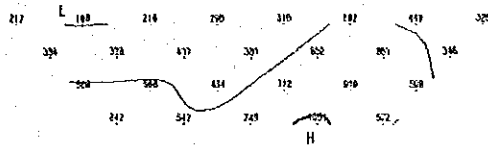


Fig.II-2-5(2) Section of apparent resistivity of the reconnaissance

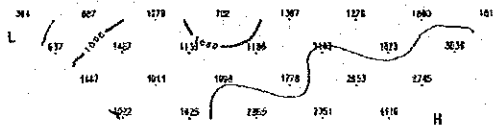
LINE-K 0 2 4 6 8 10 12 14 16 18 20



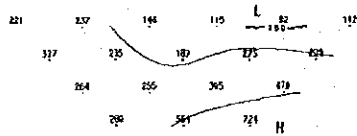
LINE-L 0 2 4 6 8 10 12 14 16 18 20



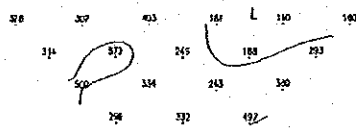
LINE-Za 0 2 4 6 8 10 12 14 16 18 20



LINE-M 0 2 4 6 8 10 12 14 16



LINE-N 0 2 4 6 8 10 12 14 16

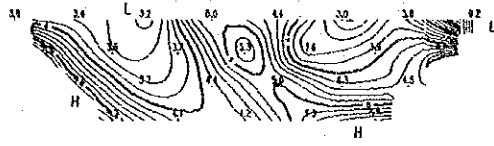


100 0 100 200 300 400 500 (metres)

UNIT: [$\Omega \cdot m$]

Fig.II-2-5(3) Section of apparent resistivity of the reconnaissance

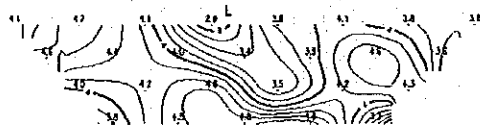
LINE-F 0 2 4 6 8 10 12 14 16 18 20



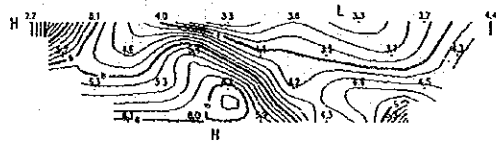
LINE-G 0 2 4 6 8 10 12 14 16 18 20 22 24 26 28



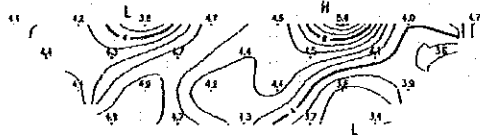
LINE-H 0 2 4 6 8 10 12 14 16 18 20



LINE-I 0 2 4 6 8 10 12 14 16 18 20



LINE-J 0 2 4 6 8 10 12 14 16 18 20



100 0 100 200 300 400 500
(meters)

UNIT: (mV/V)

Fig.II-2-6(2) Section of chargeability of the reconnaissance

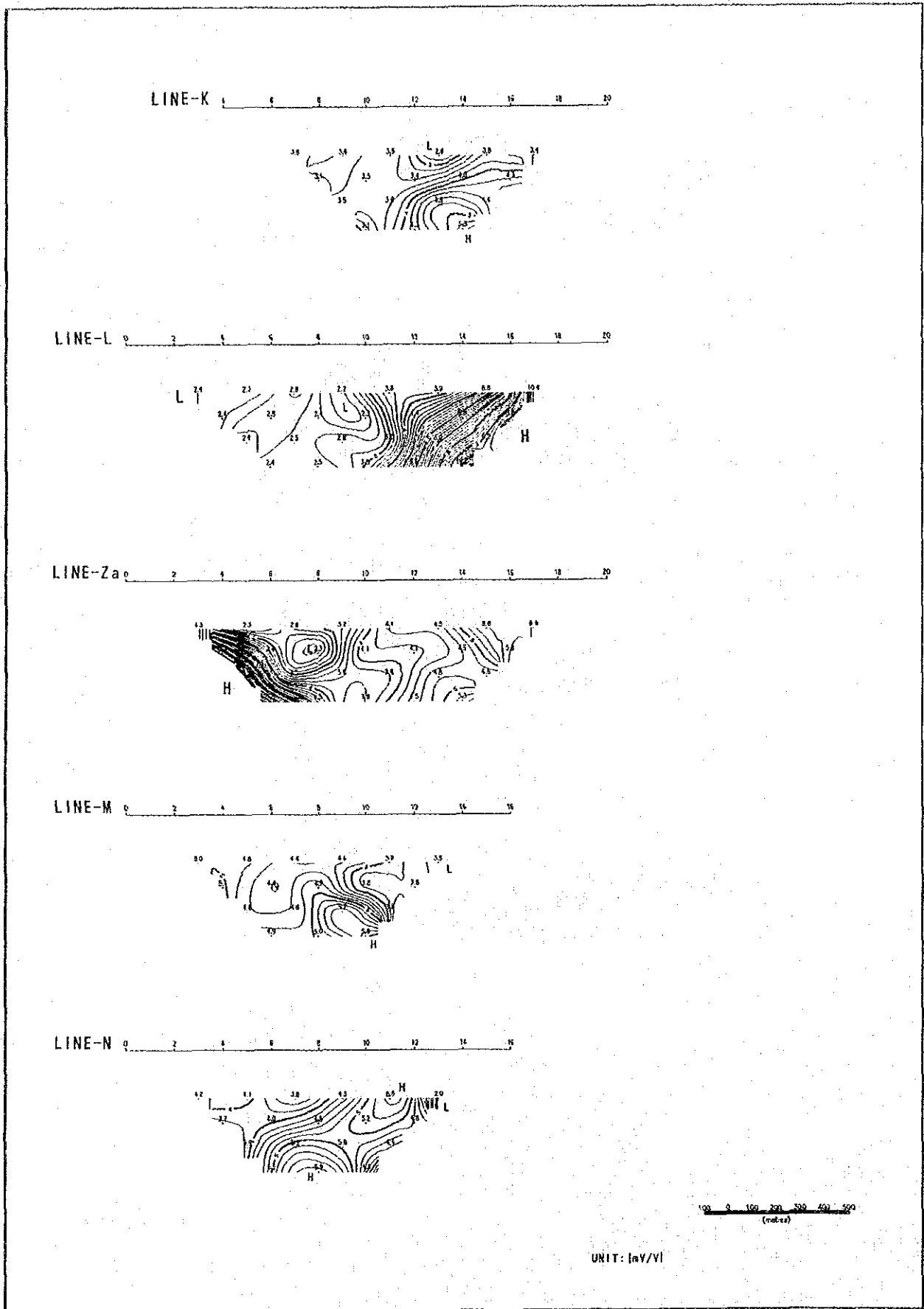


Fig.II-2-6(3) Section of chargeability of the reconnaissance

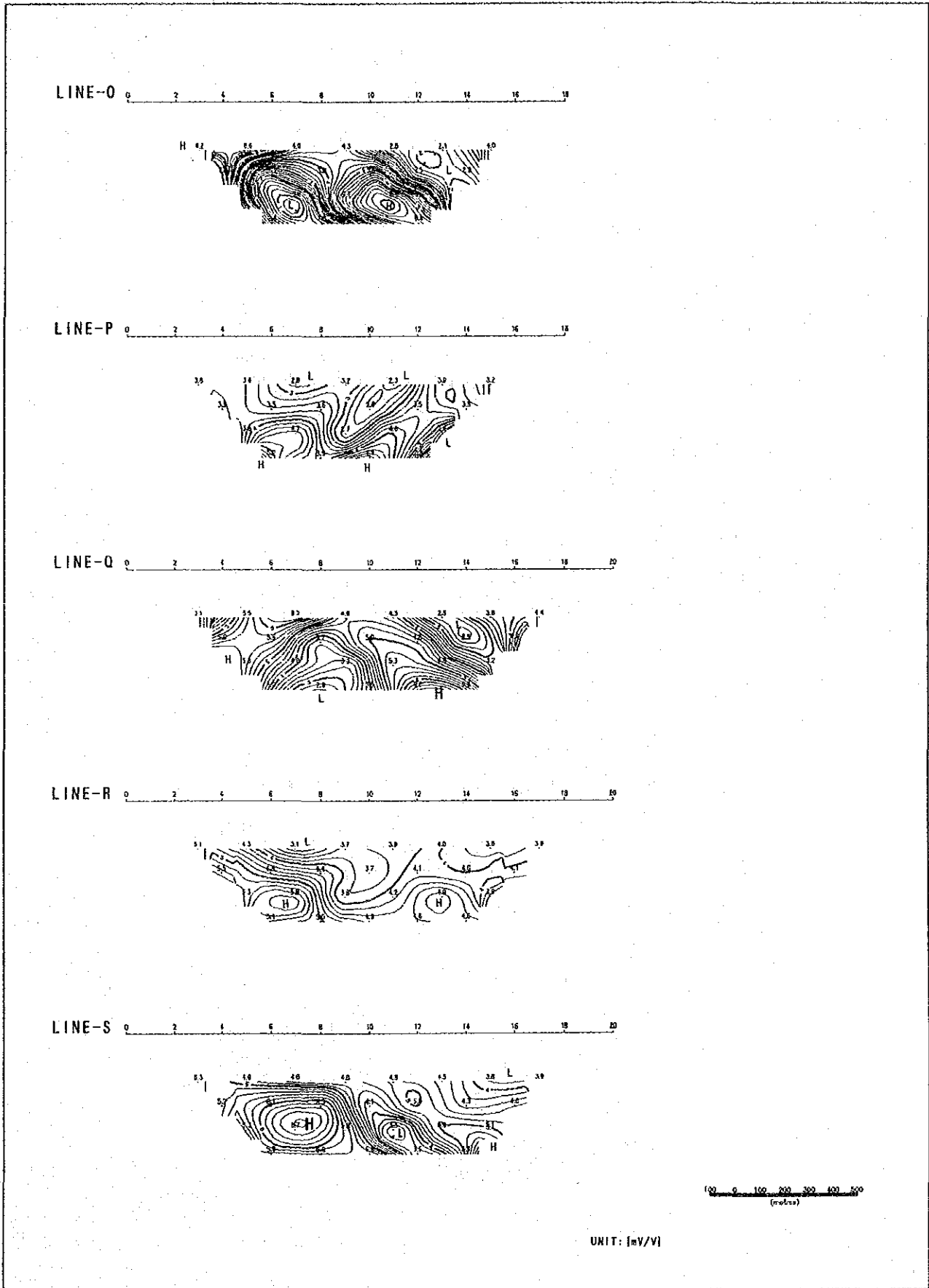


Fig.II-2-6(4) Section of chargeability of the reconnaissance

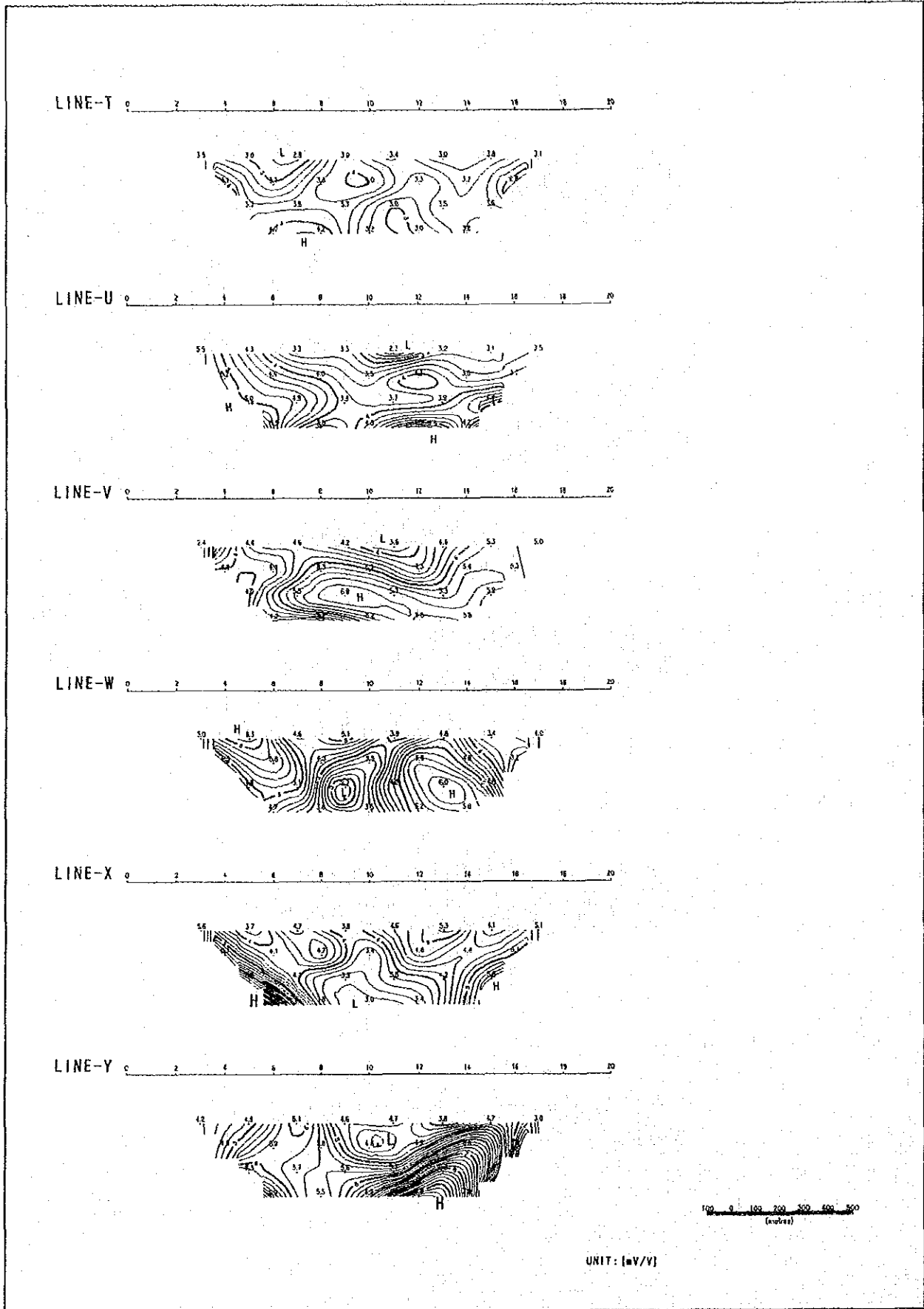


Fig.II-2-6(5) Section of chargeability of the reconnaissance

TableII-2-4 List of the results of reconnaissance

| line | Resistivity | IP value | characteristic of distribution |
|------|-------------|------------|---|
| A | 500 ~ 5,000 | 1.8 ~ 6.1 | generally low IP |
| B | 64 ~ 1,400 | 1.8 ~ 9.6 | distinct IP anomaly on stations No.2 to No.10 |
| C | 319 ~ 3,024 | 2.4 ~ 8.2 | distinct IP anomalies on stations No.2 to No.14 |
| D | 119 ~ 2,860 | 4.7 ~ 8.8 | generally indistinct |
| E | 130 ~ 3,135 | 1.0 ~ 5.0 | generally low IP |
| F | 422 ~ 3,105 | 0.2 ~ 5.8 | generally indistinct |
| G | 196 ~ 1,055 | 2.1 ~ 6.6 | generally low IP |
| H | 147 ~ 580 | 2.9 ~ 4.9 | generally low IP |
| I | 342 ~ 4,182 | 3.3 ~ 7.7 | IP anomaly in the shallow the station No.2 |
| J | 240 ~ 825 | 3.6 ~ 5.6 | generally indistinct |
| K | 175 ~ 1,054 | 2.6 ~ 5.3 | generally low IP |
| L | 198 ~ 1,051 | 2.2 ~ 10.6 | detected an IP anomaly on stations No.14 to No.20 |
| Za | 394 ~ 4,615 | 2.3 ~ 9.0 | detected an IP anomaly on stations No.0 to No.4 |
| M | 92 ~ 715 | 4.4 ~ 5.9 | weak IP anomaly, widening towards the deep part |
| N | 140 ~ 573 | 3.5 ~ 5.9 | weak IP anomaly on the stations No.10 to No.12 |
| O | 169 ~ 1,433 | 0.8 ~ 7.8 | distinct IP anomaly widening towards the deep part |
| P | 149 ~ 2,367 | 2.3 ~ 5.2 | generally low IP |
| Q | 132 ~ 769 | 2.6 ~ 6.6 | weak IP anomaly on the stations No.4 to No.14 |
| R | 172 ~ 1,236 | 3.1 ~ 5.8 | weak IP anomaly in the deep part the No.6 station |
| S | 142 ~ 4,730 | 3.8 ~ 6.7 | weak IP anomaly in the deep part the No.6 station |
| T | 230 ~ 753 | 2.8 ~ 4.2 | generally low IP |
| U | 217 ~ 1,499 | 2.3 ~ 5.5 | generally low IP |
| V | 413 ~ 2,684 | 2.4 ~ 6.0 | generally indistinct |
| W | 145 ~ 1,519 | 2.7 ~ 6.3 | weak IP anomalies on the stations No.4 and No.12 |
| X | 221 ~ 1,600 | 3.0 ~ 8.8 | detected an IP anomaly on the stations No.0 to No.6 |
| Y | 374 ~ 2,270 | 3.0 ~ 9.6 | distinct anomaly on the stations No.12 to No.16 |